

Fault Isolation of Open Defects Using Space Domain Reflectometry

Mayue Xie, Zhiguo Qian, Mario Pacheco, Zhiyong Wang, Rajen Dias
Intel Corporation, Chandler, AZ, USA

Vladimir Talanov
Neocera, LLC, Beltsville, MD, USA

Abstract

Recently, a new approach for isolation of open faults in integrated circuits (ICs) was developed. It is based on mapping the radio-frequency (RF) magnetic field produced by the defective part fed with RF probing current, giving the name to Space Domain Reflectometry (SDR). SDR is a non-contact and nondestructive technique to localize open defects in package substrates, interconnections and semiconductor devices. It provides 2D failure isolation capability with defect localization resolution down to 50 microns. It is also capable of scanning long traces in Si. This paper describes the principles of the SDR and its application for the localization of open and high resistance defects. It then discusses some analysis methods for application optimization, and gives examples of test samples as well as case studies from actual failures.

Introduction

One particular challenge of fault isolation for electronic packages is accurate localization of open defects. Such defects include cracked traces, delaminated vias, non-wet bumps, bump fractures, and other package or interconnect structures that result in device open failure. The main approach for localizing these defects today is time domain reflectometry (TDR) or similar technology. TDR sends a short electrical pulse into the device and monitors the reflections. These reflections can correspond to shorts, opens, bends in a wire, normal interfaces between devices, or high resistance defects. Ultimately, any feature associated with a change in the trace characteristic impedance produces a TDR response. Comparison of this response to that obtained on a good part allows pinpointing the failure site. Recent development in TDR technique has achieved very high signal-to-noise ratio and much improved spatial resolution [1].

For more than a decade, Magnetic Field Imaging (MFI) has been used for shorts and leakages localization in the packages [2] and dies [3]. The technique employs a Superconducting Quantum Interference Device (SQUID) sensor operating at kHz frequency. MFI for packaged devices is accomplished by measuring the vertical component of magnetic field produced by the current flowing via the short circuit. Magnetic field data are transformed into current density images, which typically show higher gradients at localized narrow current paths, or dissolution of current density where narrower paths dissipate to much broader conductors or power planes at short circuit

sites. An AC bias is utilized on the sample to enable lock-in amplification for noise reduction.

In this paper, we show that by increasing the bandwidth of the SQUID electronics into the RF range [4], MFI can find open defects in packages and dies, through imaging magnetic field in the space domain, giving the name to Space Domain Reflectometry (SDR). This paper describes the principle of the SDR and its applications for localization of physical and electrical open defects. It then discusses some analysis methods for application optimization, and gives examples of test samples as well as results of case studies from actual failures.

Fundamentals and theory of SDR

DC and low frequency signals, normally used in electrical probing of ICs, cannot induce a current flow in the interconnect structure interrupted by the open. This changes, however, if the signal frequency is brought into the RF range, where the open-circuited trace can be treated as a transmission line of characteristic impedance Z_0 terminated with the open characterized by the lumped element Z_{open} , as shown in Fig. 1.

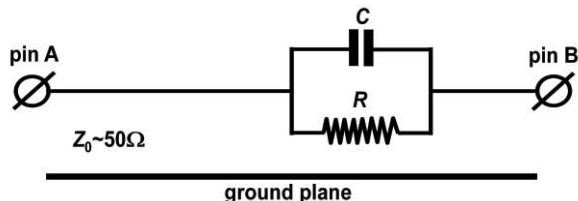


Figure 1. Lumped element representation of the open failure. Z_0 is the characteristic impedance of transmission line formed by the trace.

By modeling the open as a parallel circuit with resistance R and capacitance C , we obtain for its impedance:

$$Z_{open} = \frac{R}{1 + (\omega RC)^2} + i \frac{\omega R^2 C}{1 + (\omega RC)^2} \quad (1)$$

where ω is the angular frequency of the RF probing signal. At 100 MHz, the representative $R=1M\Omega$ and $C=1fF$ yield $|Z_{open}|$ in $M\Omega$ range.

The SDR technique injects continuous wave RF signal into a defective trace via feed-line (formed by the coaxial cable or RF probe) connected to, e.g., pin A in Fig. 1. For the

reflection, Γ , and transmission, T , coefficients of the incident probing wave one obtains

$$\Gamma = \frac{Z_{open} - Z_0}{Z_{open} + Z_0} \approx 1 - \frac{2Z_0}{Z_{open}} \approx 1$$

$$T = 1 - \Gamma \approx 0$$
(2)

where the expansion is due to $Z_0 \ll |Z_{open}|$. It is due to this condition the open reflects nearly all the incident RF power back toward the feed-line, while no RF power is transmitted past the open (e.g., toward pin B in Fig. 1). A superposition of the incident and reflected signals forms a standing wave [5], as shown in Fig. 2. The amplitude of a standing wave current along the trace can be found as follows:

$$I = 2 \sqrt{\frac{P}{Z_0}} \sin(\gamma x) \approx \sqrt{\frac{P}{Z_0}} \gamma x \propto \sqrt{P} \omega x$$
(3)

where P is the power of the RF probing signal, $\gamma = \omega \sqrt{\epsilon} / c = 2\pi / \lambda$ is the propagation constant of the trace transmission line with ϵ the effective dielectric constant, c the speed of light, and λ the wavelength, and x is the position along the trace. The open is located at $x=0$ and coincides with the rightmost node of the standing wave current. Since for typical ICs at RF frequencies $\gamma x \ll 1$ (due to IC size $\ll \lambda$), in vicinity of the open the standing wave current varies linearly due to $\sin(\gamma x) \approx \gamma x$.

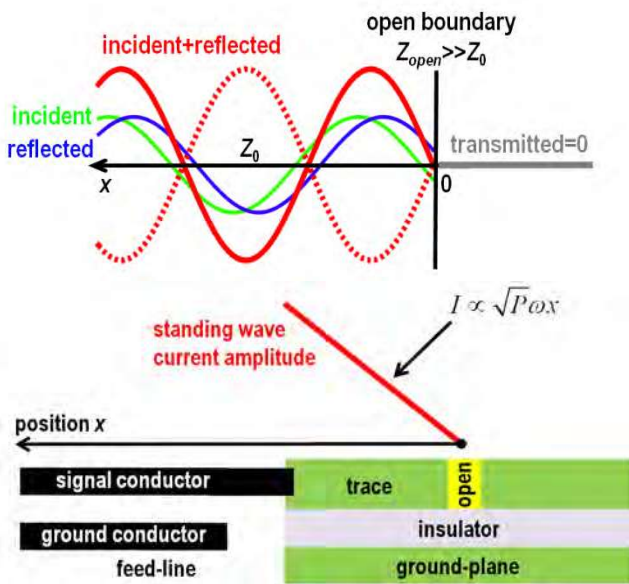


Figure 2. (a) The incident, reflected, transmitted, and standing waves in the open-circuited transmission line. Solid and dotted lines show the standing wave profiles shifted by 180°. (b) Cartoon of the

standing wave current amplitude in vicinity of the open. The feed-line signal wire is connected to the defective trace, while the ground wire may be either left floating (shown) or connected to the IC ground-plane.

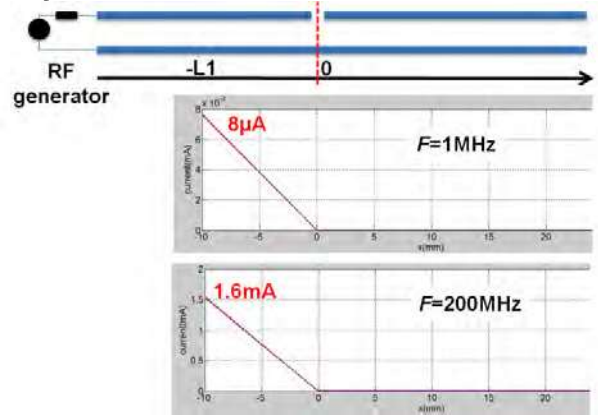


Figure 3. Modeling the standing wave current vs. probing frequency. For a fixed RF power, the standing wave current gradient is much larger at higher frequency, hence providing better resolution.

Equation (3) shows that in order to improve the open localization accuracy both the probing RF power and frequency should be made as high as practical. This was confirmed by results of numerical modeling shown in Fig. 3, where at 1 and 200 MHz the standing wave current was modeled in the open-circuited transmission line with $Z_0=50\Omega$ for $C=0.1$ and 1fF . The open was placed at $x=0$ and RF power was fed from the left hand side. One can see that at distances $x=L_1 \ll \lambda$, the ratio of the standing-wave current amplitudes $1.6\mu A / 8\mu A = 200$ equals to that of the frequencies $200\text{MHz} / 1\text{MHz}$, in agreement with Eq. (3). No dependence of the current amplitude on the open capacitance C was found due to $Z_0 \ll |Z_{open}| = 1 / \omega C$.

Experimental setup

A standard MFI microscope “Magma” was upgraded with the newly developed electronics capable of operating the SQUID over frequency range 60 to 200 MHz [4] and injecting a RF probing signal into the trace under test (Fig. 4).

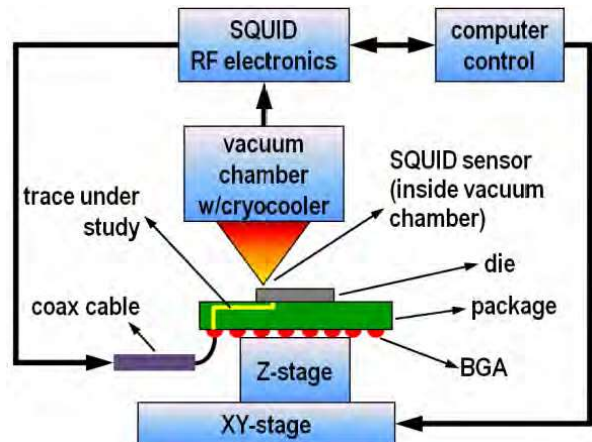


Figure 4. MFI system based on scanning SQUID RF microscope.

RF-MFI images the magnetic field of a standing wave following the failed structure to the vicinity of the open, which allows recovering the standing wave current profile and to find its node, thereby locating the open. Unlike in TDR where the failure location is identified by distance (1D) measured along the failing trace, SDR yields the failure isolation in 2D. According to the principles of near-field microwave microscopy (e.g., see [6]), SDR's spatial resolution is not limited by the frequency but rather the SQUID (probe) size and the SQUID-to-sample separation. This enables SDR to locate opens with accuracy down to 30 μm .

Results

In order to assess the capabilities and limitations of SDR technique, various kinds of open defects were evaluated and numerical simulations were carried out to better understand the defect signature and to optimize the scanning parameters.

First, as a proof of principle, we imaged a 50 Ω microstrip transmission line interrupted by the 50- μm -wide gap (open) mechanically cut across the entire microstrip (see Fig. 5). The 200MHz RF probing signal at 1mW of power was fed into the sample via standard SMA connector. The probe-to-sample separation was 100 μm . The images confirm that both the RF magnetic field (B_z) and RF current decay linearly down to zero at the open. The open was found within 50 μm from its physical location, which was limited by the open width.

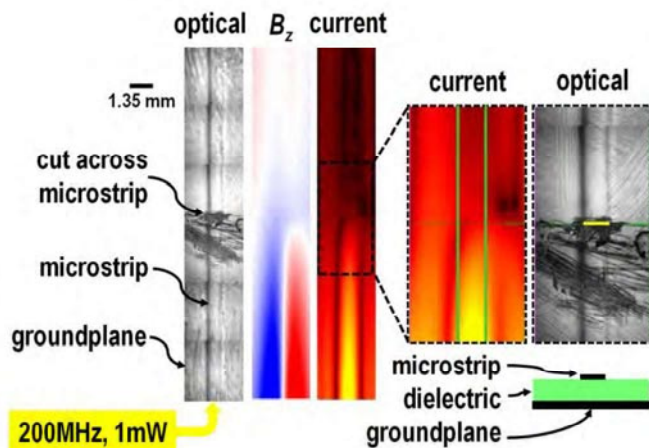


Figure 5. Imaging a microstrip transmission line with the 50- μm -wide dead open mechanically cut in the microstrip. SDR found the open within 50 μm from its physical location, limited by the open width.

Secondly, a serpentine trace structure with a laser-cut open was selected to study the SDR capability because of serpentine's dense loop design. Numerical modeling was done to understand the spatial resolution vs. scanning distance as shown in Fig. 6. It confirmed that smaller SQUID-to-sample distance, on the order of the serpentine pitch, is required to resolve very closely spaced metal traces. Analysis is also done to understand the impact of scanning frequency on the resolution as shown in figure 7. It was found that higher

frequency scanning provides better resolution with sharper current gradient before and after the open location. The serpentine trace structure was then scanned using these optimized parameters for improved resolution. Figure 7 shows the scanning magnetic field, current density distribution and optical image with failure location. Failure location comparison demonstrated a 70 μm resolution with a 50 μm scanning distance and 200MHz scanning frequency.

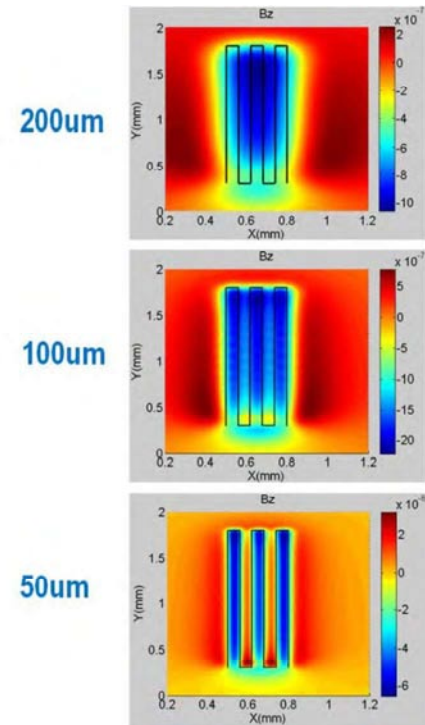


Figure 6: Modeling SDR's spatial resolution vs. SQUID-to-sample distance of 200 μm , 100 μm and 50 μm : smaller scanning distance is required to resolve very closely spaced metal traces.

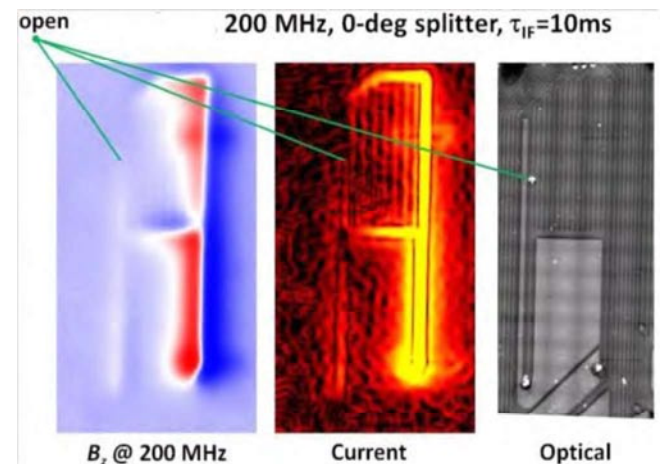


Figure 7: A sample with a serpentine open failure at one of the traces was scanned using SDR with optimized scanning parameters. The left is the magnetic field image collected by the "Magma" MFI microscope, and the middle image shows the current density distribution with open location highlighted. The optical image at the right shows the laser-created open of the trace. The open location

identified by current image is about $\sim 70 \mu\text{m}$ away from its physical location.

Case Studies

This section contains examples of successful application of the SDR technique to various open failure modes of a flip chip package. The spatial resolution of SDR on real package level failure is to be studied through these cases.

Case 1. The first real product application case is a test vehicle (TV) with a serpentine structure of finer trace-to-trace pitch. This TV failed open after extensive reliability testing. The SDR scanning distance was about 1 mm limited by the presence of the die above the package. As a result, the SDR scanning parameters were not optimized and instead used the “normal” setups, and the resolution for this case is expected to be much worse than the one shown at the previous session. The current image at the vicinity of the failure, its optical picture and actual failure location and failure mode are shown in Fig. 8. In this case, normal scan was able to isolate the failure to within a single serpentine line. However, magnetic field cancelation due to alternating flow of current in adjacent serpentine lines prevents the technique from resolving the current in a single line. Improvements using focused area scan with higher frequency and smaller steps and reduced SQUID-window distance will enable resolution improvement.

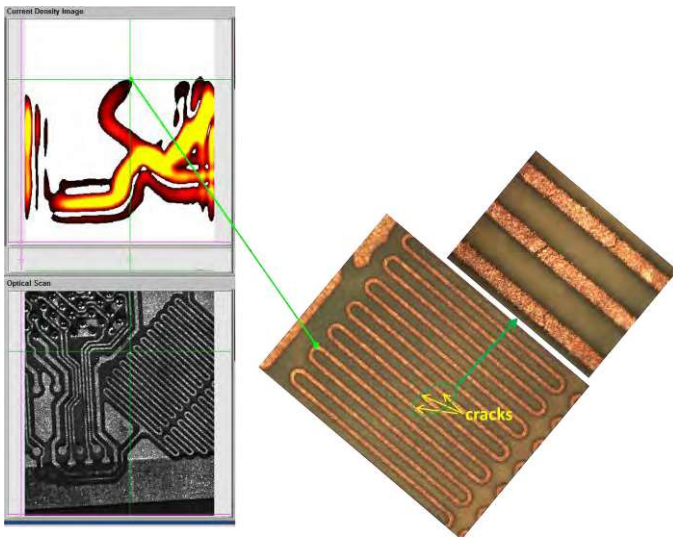


Figure 8: A sample with a serpentine open failure at one of the traces was scanned using SDR with normal scanning parameters. The top-left image shows the current density distribution with open location highlighted. The optical image at the bottom-left shows design layout of the trace structure. The right image shows the actual failure location and mode. The SDR current image identifies the first serpentine trace with crack, which is about $400\mu\text{m}$ away from its physical location.

Case 2. The second real product application case is a package with a trace cracking after extensive reliability testing. The SQUID-to-sample distance was also about 1 mm due to the presence of the die. A fast-step scanning was done to locate the approximate failure location and followed by a finer step

scan for improved location accuracy as shown by Fig. 9. The current image at the left clearly follows the trace of interest until the die edge, where the current density significantly weakens which suggests the failure is around the die edge. Physical failure analysis found a trace crack open at the vicinity current termination point as shown by the image on the right. The fact that the current does not disappear immediately after the termination point might be caused by the crowded turns of the trace and die edge effects, which are currently being investigated by software algorithm improvement. In this case, a normal MFI scan isolates the trace open within $\sim 150\mu\text{m}$.

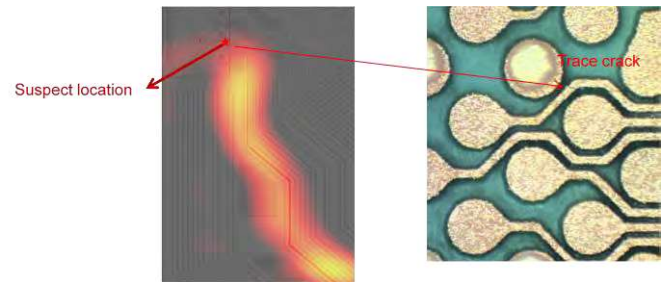


Figure 9: SDR scanning of a trace open case with normal scanning parameters. The left image shows the current density distribution with open location highlighted. The optical image at the right shows the actual trace and its failure location. In this case, the SDR scanning location accuracy is about $150 \mu\text{m}$.

Case 3. The third case is a test vehicle package with multiple C4 bump non-wet opens on a long daisy chain. The daisy chain goes up and down between the die and package, and is a good example of demonstrating tool applicability to long traces inside Si. The SQUID-to-sample distance was again about 1 mm due to the presence of the die. The 200MHz RF probing signal at 1mW of power was fed into the sample from the two ends of the daisy chain. The current density images and cross section images confirming non-wet C4 joints are shown in Fig. 10. The left hand side image is the first scan with RF signal fed from the left side of the chain. The current flow is not continuous because one segment of the trace was covered by a solid metal plate on the top layer. The right hand side image is the second scan with RF signal fed from the right side of the chain. The RF current flow clearly follows the daisy chain structure while its density decreases linearly toward the open C4 bump. Simple observation on the current density identifies that the open location is about 2 bumps away from the actual failure location. Failure isolation using linear extrapolation based on Eq. (3) was then applied to this case and successfully pinpointed the open bump. This implies that a localization accuracy of better than $70 \mu\text{m}$ was achieved for this case even with 1 mm probe-to-sample distance.

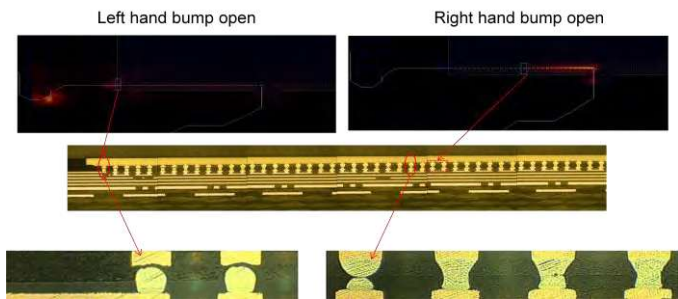


Figure 10: SDR scanning of daisy chain of multiple C4 non-wet opens with normal scanning parameters. The left image shows the current density distribution with open location at the first bump of the left side chain. The right side image shows the current density distribution with open location with inner bumps of the right side of the daisy chain. Cross section confirmed the open location with localization accuracy down to 70 μ m using the linear extrapolation algorithm.

Discussion and Conclusion

All six samples discussed in this paper are summarized in the Table 1 below. This shows that the SDR scanning works well for different package open failure modes with a resolution down to 50 μ m.

Table 1: Failure modes and localization accuracy for six cases discussed in this paper.

Case#	Failure location	Failure mode	SDR accuracy
1	Microstrip	Laser cut	50 μ m
2	Package Serpentine	Laser cut trace crack open	70 μ m
3	Package Serpentine	Multiple trace crack open	400 μ m
4	Product Package	Single trace crack open	150 μ m
5	C4-1 st bump	non-wet open	100 μ m
6	C4-Inner bump	non-wet open	70 μ m

SDR is a new non-contact and nondestructive technique that has been demonstrated to localize open defects in package substrates and interconnections. It provides a 2D failure isolation capability and complements TDR technique for more efficient failure analysis. With this 2D current image and (x, y) location, SDR eliminates the need to calculate z location with the analysis of circuit schematics. SDR has been shown to be able to localize open defects to within 50 μ m for some ideal cases and around 200 μ m for real failure application. SDR can scan long and high impedance trace by adjusting scanning frequency. As this technique is further developed to improve signal-to-noise ratio and better user experience, we expect to be able to apply it to more defect types with reduced throughput time.

Below we discuss three areas where SDR can improve to establish its unique capability as the open detection tool. The first area is to improve tool accuracy to locate the failure point more precisely and consistently. The effort includes developing an algorithm using current density linear extrapolation method, and extending it to accommodate for turns and short traces when current density is impacted by geometry discontinuity. The second area is to increase signal travel distance to account for failure detection of long traces particularly inside Si where impedance is high. As shown below in Figure 11 of signal travel distance vs signal frequency, a higher frequency signal will have more loss and travel a shorter distance on a given trace. Higher frequency scanning, however, provides better location accuracy. This imposes a challenge to optimize the tool for longer travel distance and higher resolution without increasing signal power for maximum tool applications. The third area is how to direct signal to a specific circuit branch with actual failure when there are multiple circuit branches connected to the interested chain. The tool development team has been actively looking for solutions for these challenges with progress including wider tool frequency range and better software algorithm. With its current capability on short and leakage detection, SDR is adding a unique application with increased accuracy, flexibility and capability to fill the electrical open isolation gap that the industry is facing. This will make it a versatile tool that provides solutions to a range of failure modes.

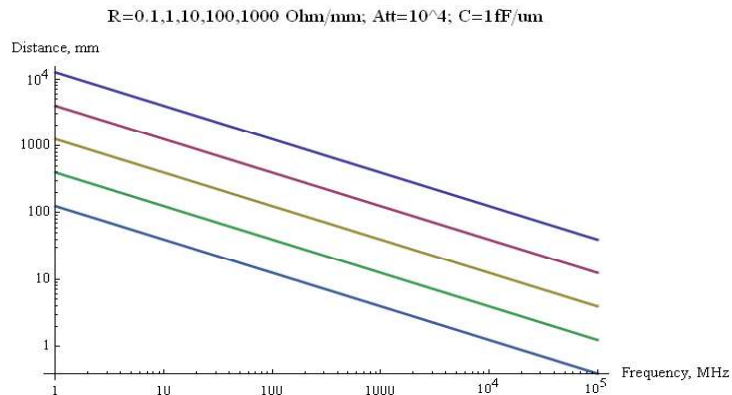


Figure 11: SDR signal travel distance vs. probing frequency: signal decays faster and travels shorter distance for higher impedance trace and higher frequency.

Acknowledgements

The authors would like to thank Dr. Antonio Orozco for fruitful discussions and Lars Skoglund, David Smith and Jan Gaustad for their sample preparation and tool support. The authors would also like to thank Deepak Goyal for his guidance and support on this project.

References

- [1] Yongming Cai, Zhiyong Wang, Rajen Dias, and Deepak Goyal, Electro Optical Terahertz Pulse Reflectometry - an innovative fault isolation tool, ECTC 2010.
- [2] R. Dias, L Skoglund, Z. Wang, and D. Smith, Integration of SQUID microscopy into FA flow, ISTFA 2001.
- [3] D. Vallett, Scanning SQUID Microscopy for die level fault isolation, ISTFA 2002.
- [4] V. Talanov, N. Lettsome, A. Orozco, A. Cawthorne, and V. Borzenets, DC SQUID RF magnetometer with 200 MHz bandwidth, 2012 APS March Meeting, February 27–March 2, 2012; Boston, MA, USA.
- [5] D. Pozar, Microwave Engineering, J. Wiley (2005)
- [6] S. M. Anlage, V. V. Talanov, and A. R. Schwartz, in *Scanning Probe Microscopy: Electrical and Electromechanical Phenomena at the Nanoscale*, eds. S. Kalinin and A. Gruverman, Springer Science, New York, 2007.